Proceedings of the 28th IEEE
EMBS Annual International Conference
New York City, USA, Aug 30-Sept 3, 2006

Estimates of Endocardial Potentials from Non-contact Intracavitary Probes

Robert Throne, Lorraine Olson, John Windle, Jeff Schweitzer, and Eric Voth

***Abstract*— The EnSite^{TM} intracavitary probe system developed by Endocardial Solutions, Inc (St. Jude Medical, St. Paul, MN) was used to simultaneously record geometric information, probe potentials, and selected endocardial potentials within the right atria for four patients. Tikhonov regularization was then used to estimate endocardial potentials from probe measurements for each patient at each endocardial site. The correlation coefficients and relative errors between the estimated potentials and the measured endocardial potentials were then calculated.**

This inverse problem was quite ill-conditioned, and first-order Tikhonov regularization performed better than zero-order or second-order Tikhonov regularization in producing stable and accurate results. In choosing the regularization parameter μ, a constant value of μ=0.3 performed as well as CRESO and Maximum Curvature, which pick a different μ for each time instant.

I. INTRODUCTION

The estimation of endocardial (interior heart surface) potentials from a probe placed in a heart chamber is one of the most promising applications of minimally invasive inverse electrocardiographic techniques. In this technique, a catheter containing a probe is inserted into a heart chamber and the probe is inflated. The probe itself is smaller than the chamber and is positioned in the blood pool without touching the heart wall. The probe surface contains many unipolar electrodes which measure the electrical potentials as a function of time. A roving contact catheter is then used to identify the three-dimensional geometry of the heart wall (endocardium). Hence, information on the geometry of the probe and its relation to the endocardium is available, along with the time-dependent probe potentials. By using inverse techniques a map of the electrical potentials on the endocardium can be obtained, which allows clinicians to more rapidly diagnose complex arrhythmias.

Because of the properties of the tissues and the time scales involved, the governing equation in the region between the probe surface and the endocardium is Laplace's equation (electrostatics). This makes the "forward problem" of calculating probe surface potentials from known endocardial potentials well-posed and stable – one boundary condition is known for each boundary and small changes in the endocardial potentials produce small changes in the probe surface potential field.

The inverse problem is far more difficult. No electrical data is available on the endocardium, and we estimate these electrical potentials based on measurements at other locations (the problem is ill-posed). The inverse problem is also ill-conditioned, and consequently small errors in the measurements cause enormous (hundreds of times larger) errors in the estimated endocardial potentials. To produce reasonable potential maps we must employ some form of "regularization", which penalizes endocardial estimates with large amplitudes or slopes.

In this study, the EnSite^{TM} intracavitary probe system developed by Endocardial Solutions, Inc (St. Jude Medical, St. Paul, MN) was used to simultaneously record geometric information, 64 probe potentials, and selected endocardial potentials within the right atria for four patients. Tikhonov regularization was then used [1] to compute endocardial potentials from probe measurements for each patient at each endocardial site. The correlation coefficients and relative errors between the estimated potentials and the measured endocardial potentials were then calculated. We then examined the level of ill-conditioning in this inverse problem, compared the performance of various orders of Tikhonov regularization, and assessed the effectiveness of various methods of choosing the regularization parameter.

II. METHODS

A. Data

We examined data for four patients– PatientA, PatientB, PatientC, and PatientD– undergoing right atrial mapping. For each patient, endocardial data was available at a number of locations, and at each location a "segment" of data (containing 2 s of data collected at 1200 Hz) was analyzed. Each segment of data, therefore, contains multiple heart beats. For PatientA, there were 21 segments; for PatientB, there were 18 segments; for PatientC, there were 13 segments; and for PatientD, there were 43 segments.

B. Finite Element Meshes

Finite element meshes were required for each patient's geometry in order to create transfer matrices $\mathbf{Z_{PE}}$ relating the probe potentials to the endocardial potentials. Figure 1 shows the finite element mesh for PatientC.

This work was supported by a grant from St. Jude Medical, Inc.

R. Throne is with the Department of Electrical Engineering, Rose-Hulman Institute of Technology, Terre Haute, IN 47803, USA robert.throne@rose-hulman.edu

L. Olson is with the Department of Mechanical Engineering, Rose-Hulman Institute of Technology, Terre Haute, IN 47803, USA lorraine.olson@rose-hulman.edu

J. Windle is Section Chief of Cardiology, Nebraska Medical Center, Omaha, NE 68198, USA jrwindle@unmc.edu

J. Schweitzer is with Endocardial Solutions, St. Jude Medical Inc, St. Paul, MN 55108, USA jschweitzer@sjm.com

E. Voth is with Endocardial Solutions, St. Jude Medical Inc, St. Paul, MN 55108, USA evoth@sjm.com

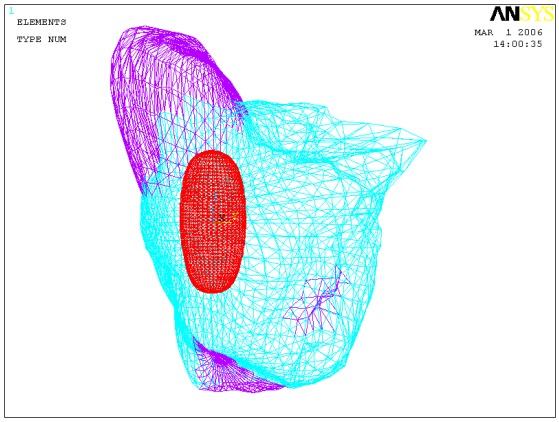

Fig. 1. Finite element mesh for PatientC. (Red: Probe. Blue: Endocardium. Purple: Superior vena cava, Inferior vena cava, Tricuspid valve.)

C. Tikhonov Regularization

The Tikhonov (TIK) regularization methods used in this study are fairly standard [1], and may be derived by minimizing a function Π

$$\Pi = ||\hat{\underline{\phi}}_P - \underline{\phi}_P||^2 + \mu||\mathbf{R}\hat{\underline{\phi}}_E||^2 \quad (1)$$

where

$\underline{\phi}_P$ = potentials measured on the probe
$\hat{\underline{\phi}}_E$ = estimate of potentials on the endocardium
$\hat{\underline{\phi}}_P$ = estimate of potentials measured on the probe
μ = regularization parameter
$\mathbf{R}$ = regularization matrix

The estimates on the endocardium and the probe are related by

$$\hat{\underline{\phi}}_P = \mathbf{Z_{PE}}\hat{\underline{\phi}}_E \quad (2)$$

If we simply minimize Π with respect to the endocardial potential estimates $\hat{\underline{\phi}}_E$ then we obtain the Tikhonov family of algorithms:

$$\left[\mathbf{Z}_{PE}^T\mathbf{Z}_{PE} + \mu\mathbf{R}^T\mathbf{R}\right]\hat{\underline{\phi}}_E = \mathbf{Z}_{PE}^T\underline{\phi}_P \quad (3)$$

When $\mathbf{R}$ is the identity matrix we are penalizing estimates with large magnitudes (zero-order regularization). When $\mathbf{R}$ is an endocardial surface gradient matrix, we are penalizing estimates with large surface gradients (first-order regularization). Similarly, when $\mathbf{R}$ is an endocardial surface Laplacian matrix, we are penalizing estimates with large surface Laplacians, which is second-order regularization. For first- and second-order regularization, one can simultaneously decompose $\mathbf{Z}_{PE}^T$ and $\mathbf{R}$ using a generalized singular value decomposition (GSVD) [2] to make the process in equation 3 more efficient, and then truncate the decomposition to improve the stability further. (Zero-order regularization requires only an ordinary singular value decomposition.) Since we have only 64 sensors on the endocardial probe, we performed the SVD/GSVD of the appropriate matrices and truncated at 64 vectors.

D. Choosing μ

Tikhonov regularization has an adjustable parameter μ which must be chosen to appropriately balance the regularization term and the match to the measured data. We examined three approaches for choosing the regularization parameter: constant values, the Composite Residual Error and Smoothing Operator (CRESO), and the maximum curvature method.

CRESO, originally proposed by Colli-Franzone [3], finds the value of μ that maximizes the difference between the derivative of the smoothing term $\mu||\mathbf{R}\hat{\underline{\phi}}_E||^2$ and the derivative of the fit to the probe surface data $||\hat{\underline{\phi}}_P - \underline{\phi}_P||^2$. This algorithm can choose a different μ value at every time instant. In practice, we must specify an initial search range for CRESO, and the algorithm is fairly sensitive to this search range and whether the range is bounded.

More recently, Hansen and O'Leary [4,5] proposed using the maximum curvature point of a log-log plot of the smoothing term $||\mathbf{R}\hat{\underline{\phi}}_E||$ versus the fit to the probe surface data $||\hat{\underline{\phi}}_P - \underline{\phi}_P||$. In our method, we use a linear-linear (not log-log) curve which is calculated for a number of μ values, then the maximum curvature is calculated by finite differences. This algorithm can also choose a different value of μ for every time instant. In practice, we must specify a search range, and a number of points within that range to examine. The algorithm is somewhat sensitive to the search range.

E. Error Measures

For each of the four patients, we generated results for various orders of Tikhonov regularization with various methods of choosing μ. We created inverse solutions for each segment for each patient, then averaged the relative errors (RE) over all segments for each patient and averaged the correlation coefficients (CC) over all segments for each patient. (Recall that the relative error can have values ranging from 0 to infinity, but small numbers are best. The correlation coefficient can have values ranging from -1 to 1, with 1 being the best value.)

III. RESULTS

We focus on three topics in examining the inverse results: whether the problem is truly ill-conditioned, what Tikhonov regularization order gives the best results, and what method for choosing the regularization parameter μ seems most effective.

A. Ill-Conditioning

Compared to the more standard inverse electrocardiography problem in which electrical potentials on the epicardium are inferred from body surface measurements [6-8] the geometry for this problem is more favorable for inverse solutions since the probe (see Figure 1) is relatively close to the endocardium.

The transfer matrix $\mathbf{Z_{PE}}$ created for each of our patients was 64×2050, relating the 64 electrodes on the probe surface to the 2050 total finite element nodes on the endocardial

TABLE I

TRANSFER MATRIX CONDITION NUMBERS

Patient	Condition Number
PatientA	1330
PatientB	920
PatientC	5260
PatientD	3170

TABLE II

GENERALIZED SINGULAR VALUES FOR GSVD DECOMPOSITION OF $\mathbf{Z_{PE}}$ AND $\mathbf{R}$ WITH FIRST-ORDER TIKHONOV REGULARIZATION.

Patient	σ_2	σ_{64}	σ_2/σ_{64}
PatientA	1.35	2.05×10^{-4}	6600
PatientB	1.56	4.99×10^{-4}	3100
PatientC	1.15	7.24×10^{-5}	16000
PatientD	1.28	9.36×10^{-5}	14000

surface. The condition numbers of the transfer matrices for the four patients studied are shown in Table I. (Here the condition number is defined in the usual way [2] as the ratio of the first singular value of $\mathbf{Z_{PE}}$ to the $64th$ singular value.) These condition numbers seem relatively modest, although they still indicate that errors in the probe measurements could be 900 to 5000 times larger when projected out to the endocardial surface using zero-order regularization.

For first- and second-order regularization, we use the GSVD of the transfer matrix $\mathbf{Z_{PE}}$ and the regularization operator $\mathbf{R}$ to perform the inverses, where the decomposition occurs simultaneously for both:

$$\mathbf{Z_{PE}} = \mathbf{UCX}^T, \tag{4}$$

$$\mathbf{R} = \mathbf{VSX}^T, \tag{5}$$

and

$$\mathbf{C}^T\mathbf{C} + \mathbf{S}^T\mathbf{S} = \mathbf{I} \tag{6}$$

Here $\mathbf{U}$ and $\mathbf{V}$ are unitary matrices, $\mathbf{X}$ is a square matrix, and $\mathbf{C}$ and $\mathbf{S}$ are nonnegative diagonal matrices. The generalized singular values σ_i of the decomposition are generally taken as the ratios of the diagonals of the matrices $\mathbf{C}$ and $\mathbf{S}$. The first singular mode for both the first-order and second-order methods is a constant (dc) over the heart surface, which is completely unaffected by the regularization matrix. Therefore, the first generalized singular value is roughly 10^7 but does not affect the solution of the problem dramatically. Consequently, Table II shows the second and last generalized singular values for first-order regularization for the four patients, which reveals the substantial ill-conditioning in the system.

B. Tikhonov Regularization of Various Orders

Tables III and IV show the results for relative error and correlation coefficient for PatientA. The correlation coefficients are similar for zero-, first-, and second-order regularization, but the relative errors are very high for zero-order regularization. (Notice that the relative error for zero-order Tikhonov reaches a minimum of 0.800 for μ=0.05, and then begins to rise again. The correlation coefficient also reaches a maximum there and then begins to drop. Therefore, we did not examine $\mu > 0.1$ for zero-order Tikhonov.) The relative errors for second-order regularization are quite high when μ is small, and the results for second-order regularization appear to be best when μ is about 50. However, even for that value the results are not as good for second-order regularization as for first-order regularization.

TABLE III

PATIENTA: RELATIVE ERRORS FOR TIKHONOV REGULARIZATION OF VARIOUS ORDERS WITH DIFFERENT CRITERIA FOR CHOOSING μ. (CRESO AND MAXIMUM CURVATURE CHOOSE A DIFFERENT μ FOR EACH TIME WITHIN EACH SEGMENT.)

μ chosen by	RE for Tikhonov Regularization		
	Zero Order	First-Order	Second-Order
μ = 0.001	1.003	–	–
μ = 0.005	0.843	–	–
μ = 0.01	0.804	–	2.515
μ = 0.05	0.800	–	1.648
μ = 0.1	0.845	0.685	1.366
μ = 0.2	–	0.648	–
μ = 0.3	–	0.635	–
μ = 0.4	–	0.631	–
μ = 0.5	–	0.630	1.006
μ = 0.6	–	–	–
μ = 0.7	–	–	–
μ = 0.8	–	–	–
μ = 1	–	0.640	0.935
μ = 5	–	–	0.799
μ = 10	–	–	0.747
μ = 50	–	–	0.682
μ = 100	–	–	0.684
μ = 500	–	–	0.682
μ = 1000	–	–	0.693
μ = 5000	–	–	–
CRESO	–	0.634	–
Maximum Curvature	–	0.637	–

Similarly, first-order regularization was substantially better than zero-order regularization and somewhat better than second-order regularization for the other three patients. In the remainder of this discussion we will focus only on first-order regularization.

Despite the ill-conditioning of the matrices, typical results for the estimated endocardial electrograms are quite good. Figure 2 shows a single beat from PatientC segment 5 using first-order Tikhonov regularization with μ=0.3, which had a relative error and correlation coefficient near the mean for that patient. Note that there is no temporal smoothing or filtering [9] employed with this algorithm, and the temporal smoothness associated with this electrode occurs simply as a result of the temporal continuity of the measured probe data.

C. Choosing the Regularization Parameter μ

Tables V and VI summarize the results for selected values of μ, for CRESO, and for the Maximum Curvature method for all patients. Recalling that low values of relative error and high values of correlation coefficient are desirable, we notice that a constant value of μ=0.3 appears to be a good choice. The relative error and correlation coefficients for CRESO are generally not as good as μ=0.3, even though

TABLE IV

PATIENTA: CORRELATION COEFFICIENTS FOR TIKHONOV REGULARIZATION OF VARIOUS ORDERS WITH DIFFERENT CRITERIA FOR CHOOSING μ. (CRESO AND MAXIMUM CURVATURE CHOOSE A DIFFERENT μ FOR EACH TIME WITHIN EACH SEGMENT.)

μ	CC for Tikhonov Regularization		
chosen by	Zero Order	First-Order	Second-Order
μ = 0.001	0.658	–	–
μ = 0.005	0.744	–	–
μ = 0.01	0.760	–	0.432
μ = 0.05	0.775	–	0.543
μ = 0.1	0.774	0.759	0.595
μ = 0.2	–	0.766	–
μ = 0.3	–	0.767	–
μ = 0.4	–	0.767	–
μ = 0.5	–	0.766	0.685
μ = 0.6	–	–	–
μ = 0.7	–	–	–
μ = 0.8	–	–	–
μ = 1	–	0.756	0.702
μ = 5	–	–	0.735
μ = 10	–	–	0.747
μ = 50	–	–	0.760
μ = 100	–	–	0.755
μ = 500	–	–	0.741
μ = 1000	–	–	0.727
μ = 5000	–	–	–
CRESO	–	0.766	–
Maximum Curvature	–	0.767	–

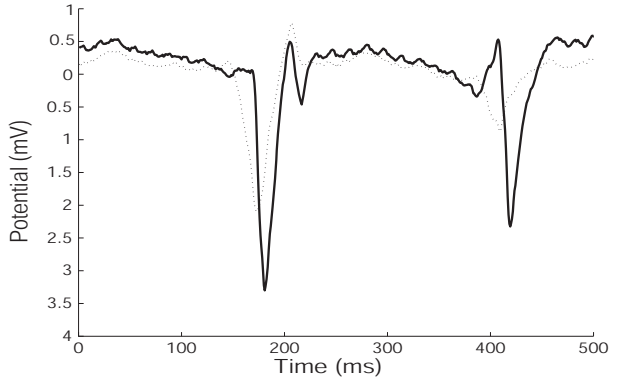

Fig. 2. Measured and Estimated Results for PatientC Segment 5. Relative Error=0.779, Correlation Coefficient=0.632. (Solid Line: Measured; Dotted Line: Estimated)

CRESO chooses a different value of μ for each time instant. Maximum curvature (with the norm of the residuals and $0.1 < \mu < 0.5$) also chooses a different μ for each time instant, but gives comparable results to the much simpler fixed μ case.

IV. CONCLUSIONS

The geometry of this inverse electrocardiography problem, with an intracavitary probe placed inside a heart chamber to predict endocardial potentials, is much more favorable than the more traditional approach which relates body surface potentials to epicardial potentials. However, the problem still demonstrates significant ill-conditioning and must be regularized. Comparing zero-, first-, and second-order Tikhonov regularization showed that first-order regularization (which penalizes the spatial slope of the endocardial potentials) was substantially better than zero-order regularization and somewhat better than second-order regularization. Of the methods considered for estimating the regularization parameter, a constant value of μ=0.3 gave the best results. Endocardial electrograms produced with first-order regularization and μ=0.3 compare well with the measured electrograms.

TABLE V

RELATIVE ERRORS FOR FIRST-ORDER REGULARIZATION FOR ALL PATIENTS WITH VARIOUS METHODS OF CHOOSING μ

	Relative Error			
Method	PatientA	PatientB	PatientC	PatientD
μ=0.1	0.685	0.875	0.854	0.860
μ=0.3	0.635	0.873	0.787	0.840
μ=0.5	0.630	0.880	0.773	0.837
CRESO	0.634	0.939	0.789	0.853
Maximum Curvature	0.637	0.879	0.771	0.839

TABLE VI

CORRELATION COEFFICIENTS FOR FIRST-ORDER REGULARIZATION FOR ALL PATIENTS WITH VARIOUS METHODS OF CHOOSING μ

	Correlation Coefficient			
Method	PatientA	PatientB	PatientC	PatientD
μ=0.1	0.759	0.505	0.586	0.587
μ=0.3	0.767	0.491	0.597	0.596
μ=0.5	0.766	0.485	0.597	0.598
CRESO	0.766	0.466	0.606	0.583
Maximum Curvature	0.767	0.487	0.604	0.595

V. ACKNOWLEDGMENTS

This work was supported by a grant from St. Jude Medical, Inc.

REFERENCES

[1] R. D. Throne, L. G. Olson, and T. J. Hrabik, "A comparison of higher-order generalized eigensystem techniques and Tikhonov regularization for the inverse problem of electrocardiography," *Inverse Problems in Engineering*, vol. 7, pp. 143–193, 1999.

[2] G. H. Golub and C. F. Van Loan, *Matrix Computations*. Johns Hopkins University Press, Baltimore, 1983.

[3] P. Colli-Franzone, L. Guerri, B. Taccardi, and C. Viganotti, "Finite element approximation of regularized solutions of the inverse potential problem of electrocardiography and applications to experimental data," *Calcolo*, vol. 22, pp. 91–186, 1985.

[4] P. C. Hansen and D. P. O'Leary, "The use of the L-curve in the regularization of discrete ill-posed problems," *SIAM Journal of Scientific Computing*, vol. 14, no. 6, pp. 1487–1503, 1993.

[5] P. Hansen, "Numerical tools for the analysis and solution of Fredholm integral equations of the first kind," *Inverse Problems*, vol. 8, pp. 849–872, 1992.

[6] B. Messinger-Rapport and Y. Rudy, "Computational issues of importance to the inverse recovery of epicardial potentials in a realistic heart-torso geometry," *Mathematical Biosciences*, vol. 97, pp. 85–120, 1989.

[7] G. Huiskamp, A. van Oosterom, and F. Greensite, "Physiologically based constraints in the inverse problem of electrocardiography," *IEEE Engineering in Medicine and Biology Conference*, 1995.

[8] F. Greensite and G. Huiskamp, "An improved method for estimating epicardial potentials from the body surface," *IEEE Trans. Biomed. Eng.*, vol. 45, pp. 98–104, 1997.

[9] R. D. Throne, L. G. Olson, and J. R. Windle, "A new method for incorporating weighted temporal and spatial smoothing in the inverse problem of electrocardiography," *IEEE Trans. Biomed. Eng.*, vol. 49, pp. 1054–1059, 2002.